Catalytic Electron Transport in *Chromatium vinosum* [NiFe]-Hydrogenase: Application of Voltammetry in Detecting Redox-Active Centers and Establishing That Hydrogen Oxidation Is Very Fast Even at Potentials Close to the Reversible H^+/H_2 Value†

Harsh R. Pershad,‡ Jillian L. C. Duff,‡ Hendrik A. Heering,‡ Evert C. Duin,§ Simon P. J. Albracht,§ and Fraser A. Armstrong*,‡

Department of Chemistry, Oxford University, Oxford OX1 3QR, U.K., and E. C. Slater Institute, BioCentrum Amsterdam, University of Amsterdam, Plantage Muidergracht 12, NL-1018 TV Amsterdam, The Netherlands

Received January 19, 1999; Revised Manuscript Received April 27, 1999

ABSTRACT: The nickel−iron hydrogenase from *Chromatium vinosum* adsorbs at a pyrolytic graphite edge-plane (PGE) electrode and catalyzes rapid interconversion of $H^+_{(aq)}$ and H_2 at potentials expected for the half-cell reaction $2H^+ \rightleftarrows H_2$, i.e., without the need for overpotentials. The voltammetry mirrors characteristics determined by conventional methods, while affording the capabilities for exquisite control and measurement of potential-dependent activities and substrate−product mass transport. Oxidation of H_2 is extremely rapid; at 10% partial pressure H_2, mass transport control persists even at the highest electrode rotation rates. The turnover number for H_2 oxidation lies in the range of 1500−9000 s^{-1} at 30 °C (pH 5−8), which is significantly higher than that observed using methylene blue as the electron acceptor. By contrast, proton reduction is slower and controlled by processes occurring in the enzyme. Carbon monoxide, which binds reversibly to the NiFe site in the active form, inhibits electrocatalysis and allows improved definition of signals that can be attributed to the reversible (non-turnover) oxidation and reduction of redox centers. One signal, at −30 mV vs SHE (pH 7.0, 30 °C), is assigned to the $[3Fe\text{-}4S]^{+/0}$ cluster on the basis of potentiometric measurements. The second, at −301 mV and having a 1.5−2.5-fold greater amplitude, is tentatively assigned to the two $[4Fe\text{-}4S]^{2+/+}$ clusters with similar reduction potentials. No other redox couples are observed, suggesting that these two sets of centers are the only ones in CO-inhibited hydrogenase capable of undergoing simple rapid cycling of their redox states. With the buried NiFe active site very unlikely to undergo direct electron exchange with the electrode, at least one and more likely each of the three iron−sulfur clusters must serve as relay sites. The fact that H_2 oxidation is rapid even at potentials nearly 300 mV more negative than the reduction potential of the $[3Fe\text{-}4S]^{+/0}$ cluster shows that its singularly high equilibrium reduction potential does not compromise catalytic efficiency.

Hydrogenases catalyze the reversible half-cell reaction $2H^+ + 2e^- \leftrightarrow H_2$ ($E = -390$ mV at pH 7.0, 30 °C, and 0.1 bar H_2) with appropriate electron donors or acceptors, and play a central role in the metabolism of a great variety of microorganisms (*1*, *2*). Interest in these enzymes is widespread and includes chemistry (*3*, *4*), microbiology (*5*, *6*), biotechnology (*7*), and evolutionary theory (*8*). The hydrogenase from *Chromatium vinosum* (*Cv*), which is isolated as a water-soluble $\alpha\beta$-heterodimer, has been studied by a variety of techniques (for an overview, see ref *1*). The larger (62 kDa) of the two subunits contains one nickel and one iron atom which are believed to constitute the active site at which $2H^+ \rightleftarrows H_2$ interconversion takes place. The smaller (32 kDa) subunit contains two [4Fe-4S] clusters and one [3Fe-4S] cluster (*9*, *10*). In vivo, the *Cv* hydrogenase is probably membrane-bound and complexed to a redox enzyme involved in the reduction of disulfides (*11*; K. L. Kovacs, personal communication). The spectroscopic characteristics are similar to those of the hydrogenase isolated from *Desulfovibrio gigas*, for which the crystal structure has been determined to 2.85 Å (*12*) and more recently to 2.54 Å resolution (*13*, *14*). The structure suggests that the three clusters $[4Fe\text{-}4S]_{prox}$, [3Fe-4S], and $[4Fe\text{-}4S]_{dist}$ provide, in sequence, an electron-transfer relay system which connects the buried NiFe center to the protein surface. However, the reduction potential of the middle [3Fe-4S] cluster is much higher than those of the two other centers, and this poses the question of its suitability as a relay center (*12*, *15*). This also raises the wider question of how important it is for relay systems in multicentered enzymes to present an uninterrupted free energy coordinate, at least on the basis of measured equilibrium reduction potentials.

† This research has been supported by the UK Engineering and Physical Sciences Research Council (Grant GR/J84809 to F.A.A.) and the Wellcome Trust (Grant 042109 to F.A.A.). S.P.J.A. acknowledges the Netherlands Organisation of Pure Research (NWO) and the Netherlands Foundation for Chemical Research (SON) for financial support.

* To whom correspondence should be addressed: Inorganic Chemistry Laboratory, South Parks Road, Oxford OX1 3QR, U.K. Telephone: +44 (0)1865 272622. Fax: +44 (0)1865 272690. E-mail: fraser.armstrong@chem.ox.ac.uk.

‡ Oxford University.

§ University of Amsterdam.

10.1021/bi990108v CCC: $18.00
Published on Web 06/23/1999

Protein film voltammetry offers attractive possibilities for studying redox enzymes (*16*−*25*, *42*, *50*). These include the ability to control driving force (electrochemical potential) over a wide and continuously variable range and to observe, simultaneously, the active sites and their engagement in catalysis. An enzyme such as hydrogenase can therefore be driven to operate in the direction of either proton reduction or hydrogen oxidation simply by application of the required potential. Provided the enzyme is able to exchange electrons rapidly with the electrode and the electroactive coverage is sufficient, then important properties of the enzyme can be investigated. In the absence of substrate turnover, redox signals corresponding to mechanistically important redox centers in the enzyme may be detected, and their reduction potentials and relative stoichiometries can be measured (*16*). Addition of substrate causes these signals to be replaced by catalytic waves, the forms of which reveal information about the kinetics and energetics of turnover (*21*). Because the diffusion field at a well-packed planar electrode surface is linear, the transport of substrates, products, and inhibitors to and from the vicinity of the enzyme can be controlled hydrodynamically, e.g., by rotating the electrode at variable high speeds (*19*−*21*). The method therefore provides an alternative perspective on complex redox enzymes, which complements and extends conventional physicochemical studies.

In this paper, we present the results of a study of *Cv* hydrogenase by protein film voltammetry. Our investigations show that *Cv* hydrogenase, when adsorbed at a PGE electrode, exhibits signals that can be assigned to some of the redox centers and exhibits extremely high activity for oxidation of H_2, which is evident even at potentials much more negative than that of the [3Fe-4S] cluster. The results provide an excellent illustration of the catalytic voltammetry of an enzyme encountered under conditions where rates approach the limit imposed by diffusion control of substrate.

EXPERIMENTAL PROCEDURES

C. vinosum (strain DSM 185) was grown as a 700 L batch culture (*26*) in a medium (*27*) essentially as described by Hendly (*28*). Cells were harvested, and the enzyme was isolated and purified as previously described (*29*). The purity of samples was checked by gel electrophoresis using an SDS−polyacrylamide (12%) gel (*30*), and protein concentrations were determined by the method of Bradford (*31*), using bovine serum albumin as a standard. The purified enzyme [contained in 50 mM Tris-HCl (pH 8.0)] was stored in liquid nitrogen. The activity for H_2 oxidation, using benzyl viologen as the electron acceptor, was 100−200 μmol min^{-1} mg^{-1}; with methylene blue, the activity was 2−3 times higher. Because of the oxygen sensitivity of the active enzyme, all electrochemical experiments were undertaken in a glovebox (Vacuum Atmospheres) under an anaerobic atmosphere, (<2 ppm oxygen) either with pure nitrogen or with 10% hydrogen in nitrogen (Air Products), as required. The thermostated electrochemical cell (*19*) was housed in a Faraday cage. A pyrolytic graphite edge (PGE) rotating disk working electrode (area of 3 mm^2) was used in conjunction with an EG&G M636 electrode rotator; a platinum wire was used as a counter electrode, and a saturated calomel electrode (SCE) in a Luggin sidearm containing 0.1 M NaCl was used as a reference. The temperature of the sidearm was measured for each experiment, and the reference potential was corrected to the standard hydrogen electrode (SHE) using a published formula (*32*). Voltammetry was performed with an Autolab electrochemical analyzer (Eco Chemie, Utrecht, The Netherlands) controlled by GPES software (Eco Chemie) and equipped with an analogue (linear) or digital (staircase) Scan Generator and an electrochemical detection (ECD) module for increased sensitivity. Unless specifically stated, all voltammograms were recorded in the digital mode, with a fractional sampling duration (α) of 0.5 and a step height (ΔE) of 2 mV (*33*). Reduction potentials of "non-turnover" signals were calculated as the average of the anodic and cathodic peak potentials, where $E^{\circ\prime} = {}^1/_2(E_{pa} + E_{pc})$. Experiments were performed using a mixed buffer system consisting of sodium acetate, MES [2-(*N*-morpholino)ethanesulfonic acid], HEPES [*N*-(2-hydroxyethyl)piperazine-*N*′-2-ethanesulfonic acid], and TAPS [*N*-tris(hydroxymethyl)methyl-3-aminopropanesulfonic acid], all purchased from Sigma, with final concentrations of 15 mM each and containing 0.1 M NaCl as an additional supporting electrolyte. All solutions were made up with purified water (Millipore, 18 MΩ cm). Mixtures were titrated with NaOH or HCl to the desired pH at the experimental temperature. To stabilize protein films, polymyxin B sulfate (Sigma) was added from a stock solution (10 g/L) to give a final concentration of 200 μg/mL. The pH values of final solutions were always checked at the experimental temperature. For each experiment, the PGE electrode was polished with an aqueous alumina slurry (Buehler, 1 μm) and sonicated thoroughly. To prepare a protein film on the electrode, either a concentrated solution of hydrogenase was applied directly onto the electrode with a capillary-drawn pipet (*34*) or the enzyme was adsorbed from dilute solution (concentrations in the range of 0.1−1.0 μM) by cycling the electrode potential between 0.242 and −0.558 V versus SHE at 100 mV/s for at least 5 min. Where necessary, the voltammetric data were smoothed using an in-house fast Fourier transform routine. The cyclic voltammograms were corrected for nonfaradic background current by subtracting a polynomial baseline (see, for example, ref *20*). Carbon monoxide-saturated solutions were prepared by bubbling 100% CO (Air Products) through a sample of the appropriate buffer/electrolyte solution for at least 20 min. The CO-saturated solution was sealed and transferred to the glovebox, and an equal volume was added to the experimental buffer solution already present in the cell. For K_M estimations, controlled volumes of 100% H_2 were piped into an N_2-filled glovebox, and the partial pressure of H_2 was estimated from the ratio of the volume of the H_2 added to the total volume of the glovebox.

RESULTS

Experiments under a Nitrogen Atmosphere. Figure 1a shows voltammograms observed over a period of 20 min after introducing a freshly polished PGE electrode to a solution of 1.0 μM *Cv* hydrogenase in buffer (pH 6.0) containing polymyxin (final concentration of 200 μg/mL, or 138 μM) at 30 °C. Successive cycles over the potential range of 242 to −558 mV versus SHE reveal the development of strong faradic features below ca. −250 mV, consisting of a sigmoidal reduction wave in the direction of decreasing potential and an intense peak-like oxidation wave on the return scan. As shown below, these features arise from proton

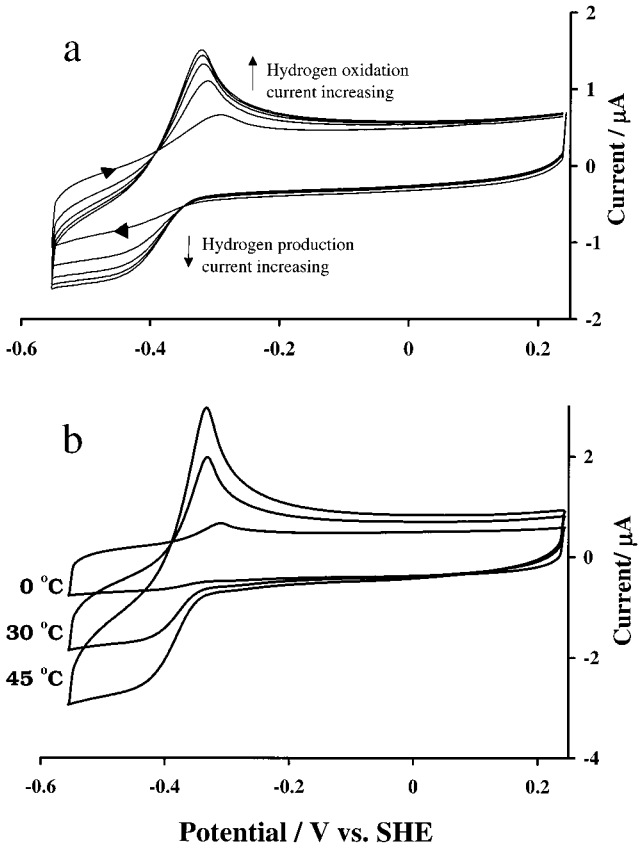

FIGURE 1: Cyclic voltammograms of *C. vinosum* hydrogenase films at a stationary PGE electrode under a nitrogen atmosphere. Panel a shows the development and stabilization of faradic activity in cyclic voltammograms recorded following immersion of a freshly polished stationary electrode in a solution containing 1 μM hydrogenase at 30 °C. The scan rate was 50 mV/s. The buffer/electrolyte solution (pH 6.0) contained 0.1 M NaCl, 60 mM mixed buffer (see Experimental Procedures), and 0.2 g/L polymyxin. Scans 2, 10, 20, 30, and 40 show an increase in the sigmoidal wave current at low potentials on the reductive scan, accompanied by an increase in intensity and the sharpness, and shift to lower potentials, of the peak-like feature on the oxidative scan. Panel b shows the voltammetric response at 0 °C and illustrates the dramatic increase in catalytic activity observed on increasing the temperature to 30 °C and then to 45 °C. The scan rate was 100 mV/s. The buffer/electrolyte solution (pH 6.8) contained 0.1 μM hydrogenase, 0.1 M NaCl, 60 mM mixed buffer, and 0.2 g/L polymyxin.

reduction and H_2 oxidation, respectively, and henceforth will be termed "catalytic" waves or peaks. No such response is observed in the absence of enzyme. Continued cycling causes the reductive wave to increase in size, the half-wave potential remaining constant during this increase, while the oxidative peak intensifies but also shifts to more negative potentials. A stable maximum response is typically achieved within 10 min. The fact that the resulting voltammetry arises from hydrogenase adsorbed at the electrode (i.e., a protein film) is easily demonstrated, since if the electrode is removed from the hydrogenase solution, rinsed, and reinserted into a hydrogenase-free solution, the faradic response persists, although with some attenuation. Similar voltammetry was observed if the concentration of the enzyme in the cell was lowered from 1.0 to 0.1 μM, but a longer time was generally required for the voltammetry to stabilize.The catalytic activity is sensitive to temperature. Figure 1b shows the voltammograms obtained after equilibrating the electrode with adsorbed hydrogenase at 0 °C and then increasing the temperature first

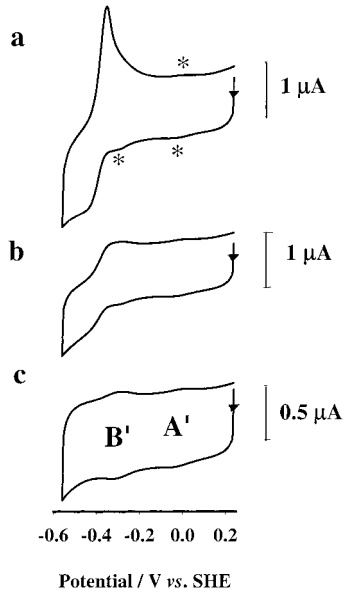

FIGURE 2: Cyclic voltammograms for *C. vinosum* hydrogenase adsorbed at a PGE rotating disk electrode. (a) Optimal analogue voltammetric responses at a stationary electrode showing catalytic activity and additionally the presence of other features, marked with asterisks. The solution, at 34 °C and pH 7.14, contained 0.1 M NaCl, 60 mM mixed buffer, 0.2 g/L polymyxin, and 0.1 mM EGTA. Hydrogenase (43 μM) was applied to the electrode using a capillary pipet. The scan rate was 100 mV/s. (b) Cyclic voltammogram recorded with the electrode rotating at 600 rpm. The intense peak on the oxidative scan is now absent. Other conditions were like those described for panel a. (c) Voltammogram recorded at a stationary electrode following addition of a CO-saturated solution. Catalytic activity is eliminated, but two pairs of redox peaks are clearly visible on both oxidative and reductive scans. Other conditions were like those described for panel a.

to 30 °C and then to 45 °C. Raising the scan rate from 10 to 100 mV/s does not noticeably affect the position or magnitude of the reductive wave, but the hydrogen oxidation peak shifts to higher potentials. In addition, the voltammetry exhibits pH dependence. Over the pH range of 5−8, lowering the pH causes both the catalytic wave and the hydrogen oxidation peak to shift to more positive potentials, and increases the magnitude of the limiting current for H^+ reduction. Some variability among separate experiments was observed, as reported also for voltammetric experiments with the Fe hydrogenase from *Megasphaera elsdenii* (*35*), but close inspection of the most intense voltammograms revealed additional features: a reductive shoulder at ca. −300 mV and a pair of oxidation and reduction peaks at ca. −30 mV versus SHE (pH 7.0). An optimal voltammogram of a hydrogenase film prepared in the presence of polymyxin is shown in Figure 2a. The additional features (denoted by asterisks) are clearly visible, and coincide with a particularly intense catalytic oxidation peak. No clear differences in the intensities of these signals were observed for films prepared by pipet-coating a concentrated layer and those prepared by adsorption from dilute solution, except that the former led to more rapid adsorption. In the absence of polymyxin, voltammograms showed lower current amplitudes, the hydrogen oxidation peak occurred at more positive potentials, and the additional features were not visible. (Polymyxin solutions alone gave a smooth featureless baseline at all times even after prolonged cycling.) The effect of rotating the electrode at 600 rpm is shown in Figure 2b. The almost

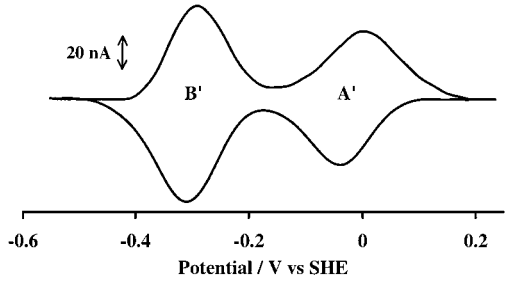

FIGURE 3: Study of redox signals in CO-inhibited hydrogenase. Baseline-subtracted voltammetric response from Figure 2c illustrating non-turnover signals A′ and B′ for the CO-inhibited enzyme. Reduction potentials in this case were -17 ± 20 and -299 ± 20 mV vs SHE (pH 7.14 and 34 °C) for A′ and B′, respectively. Experimental conditions are as given in the legend of Figure 2c.

complete disappearance of the catalytic oxidation peak confirms that it arises from a diffusible product of the reductive reaction (i.e., H_2, see below) which is swept away from the spinning electrode. The small oxidative component of the −300 mV signal is now observed more clearly, while the signal at −30 mV is unaffected. The wave that can be attributed to H^+ reduction increases just slightly and takes on a small potential dependence. As shown in Figure 2c, injection of a CO-saturated solution to the buffer/electrolyte causes the catalytic activity to disappear. This inhibition is reversible, since catalytic H^+ reduction activity is almost fully restored for the inhibited enzyme upon rapid rotation of the electrode (which has the effect of removing CO from solution). As a control, it was confirmed that CO-saturated solutions alone (i.e., free of hydrogenase) exhibit no electrochemical activity. In the CO-inhibited state, the peak-like signals at −30 and −301 mV (pH 7.0), denoted A′ and B′ respectively, persist, and these can now be examined in greater detail without the complications due to catalysis. The baseline-subtracted response is shown in Figure 3. Half-height widths were 91−108 mV for A′ and 115−126 mV for B′, which may be compared with the theoretical value of 92/*n* mV expected at 30 °C for a Nernstian redox couple involving the transfer of *n* electrons (*32*). Comparison of the peak areas using cyclic voltammetry carried out in the analogue mode (*33*) showed that the quantity of charge passed for B′ is 1.5−2.5 times that for A′. Most likely, therefore, signal B′ represents two one-electron centers having reduction potentials that are similar in value. Within reasonable error margins (±15 mV), both signals A′ and B′ are unshifted in the presence of CO. The apparent reduction potentials obtained for signals A′ and B′ are shown in Table 1, alongside relevant data from other studies. For signal A′, the separation between reduction and oxidation peaks is 5 mV at a scan rate of 5 mV/s, increasing to 50 mV at a rate of 100 mV/s. The peak separation for signal B′ is just 9 mV at a scan rate of 100 mV/s. Both sets of signals thus correspond to fast redox couples. Observed coverages varied substantially between experiments carried out under apparently identical conditions, but were typically in the range of 3−12 pmol/cm^2 [estimated on the basis (see below) that A′ is assigned to the single $[3Fe\text{-}4S]^{+/0}$ cluster]. With few exceptions, coverages lay at the low end of this range, and values at or close to 12 pmol/cm^2 (as used for Figures 2 and 3) were obtained only on very few occasions.

Experiments under a Hydrogen Atmosphere. Under an atmosphere of 10% H_2, cycling a freshly polished electrode in a dilute (1 μM) solution of hydrogenase once again produces a progressive increase in catalytic activity. In this case, the enzyme solution is preincubated in the H_2 atmosphere, and with the electrode rotating, strong sigmoidal waves develop over the course of a few minutes, i.e., a time course similar to that observed under N_2. The intense sigmoidal oxidation wave which is finally obtained reinforces the conclusion that H_2 is the oxidizable product of the experiments carried out under N_2. In control experiments, H_2-containing buffer solutions alone (i.e., without hydrogenase) exhibited no electrochemistry in the potential range studied. Figure 4a shows that the steady-state limiting current (i_{lim}) for hydrogen oxidation increases dramatically as the electrode rotation speed is increased, thus showing immediately that the catalytic rate is controlled by transport of H_2 to the enzyme layer. No clear variation in the limiting H_2 oxidation current at any given rotation rate could be established as a function of pH in the pH range of 5−8. However, as remarked previously for results obtained under an N_2 atmosphere, decreasing the pH causes the catalytic wave to shift to more positive potentials and the limiting H^+ current increases slightly.

Table 1: Comparison of Published Reduction Potentials Determined by EPR Spectroscopy with Values Determined by Film Voltammetry[a]

assignment	*E* vs SHE (mV)	pH	*T* (°C)	bacterium	ref
$[3Fe\text{-}4S]^{+/0}$	10 ± 20	7.0	30	*C. vinosum*	*29*
	-10 ± 20	8.0	30	*C. vinosum*	*29*
	-30 ± 20	7.0	30	*C. vinosum*	this study
	-33 ± 20	8.0	30	*C. vinosum*	this study
	-35 ± 20	7.0	20	*D. gigas*	*49*
$[4Fe\text{-}4S]^{2+/1+}_{prox}$	-340 ± 20	7.0	25	*D. gigas*	*47*
$[4Fe\text{-}4S]^{2+/1+}_{dist}$	-290 ± 20	7.0	25	*D. gigas*	*47*
$2[4Fe\text{-}4S]^{2+/1+}$	-301 ± 20	7.0	30	*C. vinosum*	this study
$2[4Fe\text{-}4S]^{2+/1+}$	-317 ± 20	8.0	30	*C. vinosum*	this study
"Ni_a(I)/(0)" ($n = 2$)	-458 ± 15	8.0	30	*C. vinosum*	*38*
"$N_{ir,u}$(III)/(II)"	-75 ± 20	7.0	30	*C. vinosum*	*29*
X/X^-	220 ± 20	7.0	30	*C. vinosum*	*29*

[a] prox and dist refer to the positions of the two [4Fe-4S] clusters relative to the active site (*12*).

Figure 4b is a Koutecky−Levich (K−L) plot which relates the limiting currents (as shown in Figure 4a) to the square root of rotation rate in a reciprocal manner according to eq 1 (*19*).

$$1/i_{lim} = (C + K_M/nFA\Gamma k_{cat}C) + 1/(0.62nFAD^{2/3}\nu^{-1/6}C\omega^{1/2}) \quad (1)$$

where C represents the solution concentration of H_2, n refers to the number of electrons passed per H_2 molecule consumed (here $n = 2$), F is Faraday's constant, Γ is the surface coverage of electroactive enzyme, A is the electrode area, D is the diffusion coefficient of H_2, ν is the kinematic viscosity of water, and ω is the electrode rotation rate. The constants K_M and k_{cat} are the standard Michaelis−Menten parameters.

The intercept of a K−L plot corresponds to the current extrapolated to infinite rotation rate, i.e., at which mass transport to the planar electrode surface is no longer a rate-limiting factor. Since the hydrogen concentration greatly exceeds K_M (see below), this intercept yields the turnover number k_{cat} once normalized with respect to the electroactive

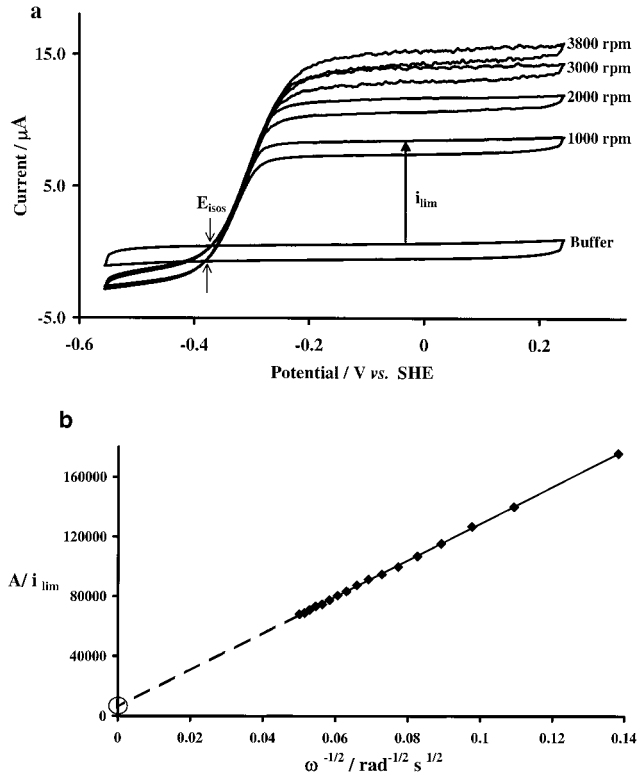

FIGURE 4: Cyclic voltammograms for *Cv* hydrogenase adsorbed at a PGE rotating disk electrode under an atmosphere of 0.1 bar H_2. (a) Cyclic voltammograms recorded at various rotation rates for a hydrogenase film at pH 6.5 and 30 °C. For comparison, the hydrogenase-free response is also included. The scan rate was 100 mV/s. The solution, equilibrated under 0.1 bar H_2, contained 0.10 M NaCl, 60 mM mixed buffer, 0.1 μM hydrogenase, and 0.2 g/L polymyxin. Increasing the rotation rate increases the observed limiting current (i_{lim}) for hydrogen oxidation (as defined in the figure). (b) Determination of k_{cat} for *Cv* hydrogenase using a Koutecky−Levich plot of data depicted in panel a. The dashed line represents extrapolation to an infinite rotation rate ($\omega^{-1/2} = 0$) to allow an estimate of k_{cat} (see the text).

coverage of the enzyme. The resulting values of k_{cat} lie between 1500 and 9000 s^{-1} over the pH range of 5−8. The errors arise from (a) the extremely high rotation rate dependence which results in a very steep K−L plot, and produces a small intercept that is difficult to define precisely, and (b) the uncertainty in coverage (see the Discussion). We were unable to obtain a reliable profile for changes in k_{cat} as a function of pH.

Certain other features of the voltammogram observed under H_2 are relevant. First, despite exhaustive searching, the non-turnover signal A′, expected now to lie on the limiting current plateau, could not be detected, even after making allowances for the lower gain used with the higher currents. Second, the isosbestic potential, E_{isos} (through which successive cycles pass as the signal amplitude increases or diminishes), defines the potential at which no *net* catalytic current flows, and therefore marks the reduction potential imposed by the solution species $H^+_{(aq)}$ and H_2 (*22*). In Figure 4a, which shows voltammograms recorded for a fully developed film, E_{isos} is simply the position at which the trace from the catalytic voltammogram crosses that of the control experiment conducted without enzyme. Values of E_{isos} for the anodic and cathodic scans were typically separated by 2−15 mV, regardless of pH or scan rate (up to 100 mV/s). As shown in Figure 5, the average values of E_{isos} (i.e., average

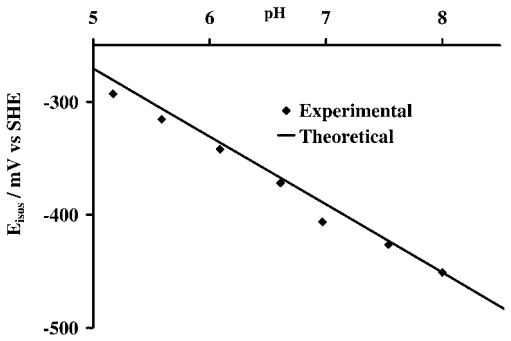

FIGURE 5: Dependence of isosbestic potential on pH. Graph showing how the isosbestic potential, the potential at which no net current flows, varies with pH. The plotted data (◆) represent the average of oxidative and reductive scans, taken from data at 30 °C, recorded in solutions under 0.1 bar H_2, containing 0.1 M NaCl, 60 mM mixed buffer, and 0.2 g/L polymyxin. The line shows the theoretical pH dependence of the reduction potential of the $2H^+/H_2$ couple under these conditions predicted by the Nernst equation.

of reductive and oxidative scans) recorded under steady-state conditions exhibited a pH dependence of -57 ± 3 mV per pH unit at 30 °C, compared to the expected value of −60 mV, and for any given pH agree well with those calculated for the reduction potential of the $H_2/2H^+$ couple according to the Nernst equation, using a $p(H_2)$ of 0.1 bar. Third, the *n* value obtained from the slope of a Heyrovsky−Ilkovich plot of $\log[(i_{lim} - i)/i]$ versus *E* increases to approach 2.0 as the rotation rate is decreased. This is as expected for voltammetry that is controlled by the mass transport of H_2 (a two-electron reductant) (*21*).

When measured manometrically using redox dyes, K_M (for the enzyme in solution) lies in the region of a few micromolar H_2 (*1*). To estimate electrochemically the K_M value for H_2 for *adsorbed* enzyme, we studied the oxidation currents observed for a range of solution concentrations of hydrogen. High oxidation currents (e.g., >2 μA at a rotation rate of 1000 rpm) were found even with a hydrogen partial pressure as low as ca. 0.01 bar (which corresponds to ca. 8 μM dissolved H_2). Again, the high rotation rate dependence prevented determination of reliable (extrapolated) limiting currents from Koutecky−Levich plots. However, on the basis of the actual current magnitudes observed even at low H_2 levels, we estimate an upper limit for K_M for the adsorbed enzyme on the order of 10 μM, in line with the solution experiments.

DISCUSSION

Considering first the cyclic voltammograms of a *Cv* hydrogenase film under N_2, the results are fully consistent with the sigmoidal wave at low potentials arising from proton reduction. Oxidation of the evolved hydrogen is then responsible for the intense peak-like feature on the oxidative scan, which disappears almost completely when the electrode is rotated. The sharp and intense appearance of this catalytic response, without the need to apply any excessive driving force (overpotential) either to produce H_2 or to reoxidize it, demonstrates that hydrogenase can exchange electrons easily in both directions with a PGE electrode. The observation that electroactivity can be transferred with the electrode to a cell free of hydrogenase shows that the enzyme is adsorbed at the electrode.

After introduction of a freshly polished electrode to an enzyme solution, electroactivity develops over the course of several cycles. Most [NiFe]-hydrogenases are inactive in the oxidized (aerobic) state, and require activation by reduction, typically by incubation under H_2 (*36*). Studies of the [NiFe]-hydrogenases from *Cv* and *Methanobacterium thermoautotrophicum* (*29*, *37*, *38*) have each shown that the redox properties of the NiFe center are very different in the inactive and active states of the enzymes. These states interconvert extremely slowly at 0 °C, and only the active enzyme is in direct redox equilibrium with H_2 or can bind CO (*38*). Importantly, experiments conducted in a nitrogen atmosphere with 10% H_2, in which the enzyme stock sample had already been incubated for several hours at 50 °C, showed a similar time lapse before reaching optimum activity. Therefore, the development of voltammetry over successive cycles appears not to be controlled by activation but, rather, by the physical adsorption processes that produce an active film.

Polymyxin, a bacterial antibiotic containing several amino groups within a cyclic polymer, stabilizes the adsorption of many proteins at PGE electrodes, yielding electroactive films often equivalent to monolayer coverage, in which the characteristic properties of the protein are retained (*34*). The stabilization is probably electrostatic and involves the polycationic coadsorbate forming noncovalent cross-linkages (salt bridges) among the negatively charged surfaces of enzyme molecules and the electrode surface. In studies of *Desulfovibrio vulgaris* (Hildenborough) hydrogenase, poly-L-lysine was found to promote enzyme adsorption onto a basal plane graphite electrode in a similar manner (*39*). The sharpened shape of the hydrogen oxidation peak and its shift toward the reversible potential, observed for *Cv* hydrogenase in the presence of polymyxin, conform well to the theoretical expectations for the effect of increasing enzyme coverage on the mode of substrate diffusion (*40*, *41*). In the microscopic model for enzyme voltammetry, diffusion-controlled electrocatalysis at well-isolated enzyme molecules adsorbed on a stationary planar electrode gives the same steady-state sigmoidal voltammograms that are observed for a microelectrode array. By contrast, a densely packed and very active film close to monolayer coverage at a stationary electrode creates the conditions for substrate depletion and produces a sharp peak-type response (*40*, *41*). This indeed correlates with the appearance of the non-turnover signals as discussed next.

The occurrence of the sharpest H_2 oxidation peak (in the presence of polymyxin), which is associated with the densest packed enzyme film, coincides with the appearance of the most prominent nonturnover signals: signal A′ at ca. −30 mV versus SHE and signal B′, a shoulder-like feature at ca. −300 mV, just positive of the catalytic waves at pH 7. These features persist as peaks when the electrode is rotated, showing that they arise from adsorbed species. This provides compelling evidence that signals A′ and B′ correspond to specific enzyme redox sites in the active enzyme, visible only at the densest coverage of enzyme on the electrode. Put another way, the electrocatalytic activity is so high that it is very unlikely that it could arise from an electrode which is only sparsely populated with active enzyme; consequently, non-turnover signals certainly ought to be visible even if faint. On the basis of the above assignments, integration of signal A′ gave coverage values ranging up to 12 pmol/cm^2. We may make comparisons with other enzymes for which film voltammetry has so far proved to be successful, where the visibility of non-turnover signals is accompanied by a sharp, peak-like catalytic response when the electrode is stationary. Fumarate reductase (FrdAB) from *Escherichia coli*, a two-subunit enzyme which has a mass (93 kDa) very similar to that of *Cv* hydrogenase, gives a saturating electroactive coverage of ca. 3 pmol/cm^2, which equates to an area of ca. 5600 Å^2 per enzyme molecule based upon a ideal flat electrode (*19*, *20*). Flavocytochrome c_3 from *Shewanella frigidimarina* (64 kDa) saturates at 9 pmol/cm^2 (*42*), while yeast cytochrome *c* peroxidase (34 kDa) gives coverages in the range of 3−6 pmol/cm^2 (*24*, *25*). In all these cases, electroactive protein coverage fluctuates from one experiment to another, and the variations observed here with hydrogenase, although larger, are not unexpected. The factors controlling protein interactions with electrode surfaces are recognized to be complex (*43*, *44*). Inhomogeneity among adsorbed enzyme molecules may produce appreciable dispersion and render non-turnover signals difficult to observe (*45*). Even in the absence of dispersion, we consider that below 3 pmol/cm^2, a one-electron signal such as A′ might escape detection by analogue cyclic voltammetry. Conversely, 12 pmol of hydrogenase/cm^2 on a geometrically flat surface would be equivalent to an area of ca. 1400 Å^2 per molecule. In comparison, the crystal structure suggests a cross-sectional area of ca. 2800 Å^2 for *D. gigas* hydrogenase (*13*) so that this high coverage could only be accommodated with a microscopically rough electrode surface or secondary layer enzyme molecules that remain electrochemically active, perhaps by rapid interchange processes.

Catalytic proton reduction and oxidation of the generated H_2 dominate the low-potential region and partly obscure signal B′. Whereas for hydrogenase it is not possible to eliminate one of the substrates (H^+) from aqueous solution, inhibiting the enzyme with carbon monoxide [$K_i \sim 25$ μM (our own unpublished measurements)] facilitates the observation of signal B′ and enables it to be compared with signal A′ in terms of shape and stoichiometry. From their small peak separations (the difference between oxidation and reduction peak potentials), signals A′ and B′ are each associated with centers capable of fast redox cycling uncomplicated by gating effects. No other non-turnover signals were observed for a CO-inhibited enzyme over the potential range of 242 to −758 mV versus SHE.

The reduction potentials of the two [4Fe-4S]$^{2+/1+}$ clusters in *Cv* hydrogenase have not as yet been determined potentiometrically, since the reduced 3Fe cluster ($S = 2$) prevents study of the [4Fe-4S]$^+$ clusters due to severe line broadening of their EPR signals. Table 1 compares the reduction potentials of the redox couples observed by film voltammetry with literature values for identified redox centers, based on potentiometric titrations monitored by EPR spectroscopy. According to EPR, the active site-inhibited "Ni(II)−CO" state does not undergo redox changes upon adding either 2,6-dichlorophenolindophenol ($E^{\circ\prime} = 230$ mV) or dithionite [$E^{\circ\prime} = -531$ to −473 mV for concentrations of dithionite from 10 μM to 1 mM respectively (*46*)] (*1*). Noting that both signals A′ and B′ appear to be unaffected by CO, and by analogy with *D. gigas* [NiFe]-hydrogenase (*47*), we propose that signal B′ is due to at least one and probably both of the [4Fe-4S]$^{2+/1+}$ clusters in the *Cv* enzyme. Small

differences are commonly observed when comparing reduction potentials measured potentiometrically for bulk solution versus direct electrochemical measurement on a protein film. Thus, signal A′ ($E^{\circ\prime} = -33 \pm 20$ mV at pH 8.0 and 30 °C) most likely corresponds to the [3Fe-4S]$^{+/0}$ couple, the potentiometric value of which is -10 ± 20 mV under comparable conditions.

The cyclic voltammograms obtained under H_2 atmospheres (1−10%) show clearly that the current due to hydrogen oxidation is very sensitive to rotation rate, and thus mass transport-controlled, whereas only a small dependence on rotation rate is observed for proton reduction. Indeed, mass transport control of H_2 oxidation persists up to the highest possible electrode rotation rates. Even when the errors involved in determining the electroactive coverage of the intercept on the K-L plot are considered, the range of k_{cat} values (1500−9000 s^{-1}) is significantly greater than values reported using oxidants such as benzyl viologen (300 s^{-1}) or methylene blue (650−900 s^{-1}) despite the high driving force ($E = 11$ mV vs SHE) provided by the latter. As discussed, K_M for H_2 for the adsorbed enzyme lies in the approximate range of 1−10 μM, consistent with measurements with enzyme in solution (*1*). Thus, we expect a second-order rate constant k_{cat}/K_M of the order of 10^8-10^9 M^{-1} s^{-1}, which fully upholds our experimental observation that catalysis is diffusion-controlled. The extremely high activity and comparable low K_M value provide compelling evidence that the essential structural aspects of the enzyme are unperturbed by the electrode environment. The pH dependence and absolute values of the isosbestic potential E_{iso} are in good agreement with the theoretical value for the $H_2/2H^+$ couple at 30 °C and 0.1 bar H_2, so this value provides a useful in situ reference for the electron transport energetics. Over the entire pH range, the catalytic action is dominated by the oxidation current, thus immediately confirming the results of conventional experiments which also show that the enzyme is biased to function in the direction of H_2 oxidation. Comparison may be made with the results reported recently by Butt and co-workers on the Fe-only hydrogenase from *M. elsdenii*, which is biased instead toward proton reduction (*35*). In both these cases, and in other studies carried out with mitochondrial succinate dehydrogenase (*22*, *23*, *50*), the voltammetric method provides a direct measure of catalytic bias.

We can now comment on the nature of the electron transfer between the electrode and the NiFe center. On the basis of the structure of hydrogenase from *D. gigas*, this center is buried at least 25 Å below the protein surface (*11*), and fast direct electron exchange with the electrode is unlikely. The other options require that electrons exit the enzyme via the Fe−S clusters, i.e., somewhere along the chain defined by [4Fe-4S]$_{prox}$, [3Fe-4S], or [4Fe-4S]$_{dist}$. The observed electrochemical reversibility of the nonturnover voltammetric signals necessitates fast redox transitions and means that all these centers communicate with the electrode, either directly or via each other (*16*). These clusters lie at least 15, 9, and 5 Å, respectively, below the closest surface residues. The fact that [4Fe-4S]$_{prox}$ is also significantly buried further suggests strongly that electrons must exit at either [4Fe-4S]$_{dist}$ or [3Fe-4S]. We are thus in a position to qualify the role of the [3Fe-4S]$^{+/0}$ cluster whose unusually high reduction potential ($E^{\circ\prime} = -30$ mV) raises the question of whether it undergoes formal changes in oxidation level during turnover, or is indeed involved at all in intramolecular electron transport. Aside from the estimates of k_{cat} which depend on extrapolation to an infinite rotation rate, the voltammograms provide a direct measurement of catalytic rates as a function of applied potential (driving force). From inspection of the voltammograms shown in Figure 4a, we see that at the highest rotation rates used, the catalytic electron-transfer rate must lie between 400 and 1700 s^{-1} at a potential of −200 mV, i.e., 170 mV *more negative* than that of the [3Fe-4S]$^{+/0}$ couple. Such catalytic efficiency, despite the presence of an energetically uphill relay step, is further demonstrated by the simple cyclic voltammograms made with the stationary electrode under N_2 (as in panels a and b of Figure 1) in which H_2 generated on the preceding reductive scan is efficiently scavenged at a potential of ca. −300 mV, i.e., 270 mV more negative than that of [3Fe-4S]$^{+/0}$.

To date, the *Cv* [NiFe]-hydrogenase represents the most active enzyme for which a film voltammetry study has been reported, and provides an interesting example of the restrictions that may therefore arise in applying this method to the study of electron-transport enzymes. The persistence of mass-transport control, while serving to provide a very strong case for the remarkable activity that may be achieved at an electrode, masks some of the characteristic enzyme features that might otherwise be measured. As an example, during H_2 oxidation, we were unable to observe the non-turnover signals A′ and B′. Signal B′ would obviously lie within the major slope of the sigmoid, but it is not intuitively clear why A′ should not be visible. If it is assumed that signal A′ is due to [3Fe-4S]$^{+/0}$, then its apparent absence during mass transport-controlled H_2 oxidation supports the notion either that rapid catalytic redox cycling causes the signal to become less coherent or that its reduction potential shifts to a much lower value when the enzyme is undergoing turnover (*48*). The fact that its measured reduction potential is far higher than those of the other centers clearly does not compromise the enzyme's high activity. This is consistent with recent activity measurements on the P238C mutant of *Desulfovibrio fructosovorans* [NiFe]-hydrogenase (*15*). In that experiment, the mutant enzyme, which contains a [4Fe-4S]$^{2+/1+}$ cluster ($E = -250$ mV) in place of the [3Fe-4S]$^{+/0}$ cluster ($E = 65$ mV), exhibits only a minor decrease and increase, respectively, in the rates of hydrogen uptake and production, despite the improved matching of the reduction potentials of the cofactors.

CONCLUSIONS

Film voltammetry experiments carried out under a hydrogen-containing atmosphere reveal that the hydrogenase from *C. vinosum* has a remarkably high catalytic hydrogen oxidation activity, which is close to diffusion-controlled. Even with the densest electrode coverages we can postulate as reasonable, $k_{cat} > 1500$ s^{-1}, and with a K_M of ≤ 10 μM, k_{cat}/K_M is on the order of 10^9 M^{-1} s^{-1}. Although reproducibility was difficult to achieve, coated electrodes giving the sharpest catalytic peaks (under N_2) (i.e., highest coverages) also reveal non-turnover signals which persist unshifted (and somewhat clearer) when CO is added. These signals, A′ and B′, occur at -30 ± 20 and -301 ± 20 mV, respectively (pH 7.0 and 30 °C). Comparison with literature values determined by EPR measurement with redox dyes suggests

that A′ and B′ originate from the $[3Fe\text{-}4S]^{+/0}$ and the two $[4Fe\text{-}4S]^{2+/1+}$ redox couples, respectively. Our observation that oxidation of H_2 is very rapid even at potentials much lower than the formal potential of the $[3Fe\text{-}4S]^{+/0}$ cluster shows that the apparent uphill step in intramolecular electron transfer does not prevent high-level catalytic performance (*15*).

ACKNOWLEDGMENT

Mrs. T. van der Spek and Mr. W. Roseboom are acknowledged for their help with the enzyme preparation. We thank Dr. Judy Hirst, Dr. Madhu Mondal, and Miss Kerensa Heffron (GSOH) for valuable discussions.

REFERENCES

1. Albracht, S. P. J. (1994) *Biochim. Biophys. Acta 1188*, 167−204.
2. Frey, M. (1998) *Struct. Bonding (Berlin) 90*, 97−126.
3. Darensbourgh, D. J., Reibenspies, J. H., Lai, C.-H., Lee, W.-Z., and Darensbourgh, M. Y. (1997) *J. Am. Chem. Soc. 119*, 7903−7904.
4. Hsu, H.-F., Koch, S. A., Popescu, C. V., and Münck, E. (1997)- *J. Am. Chem. Soc. 119*, 8371−8372.
5. Friedrich, B., and Schwartz, E. (1993) *Annu. Rev. Microbiol. 47*, 351−383.
6. Vignais, P. M., and Toussant, B. (1994) *Arch. Microbiol. 161*, 1−10.
7. Daimler-Benz (1997) Environmental Report, Daimler-Benz, Stuttgart, Germany.
8. Martin, W., and Müller, M. (1998) *Nature 392*, 37−41.
9. Van der Zwaan, J. W., Albracht, S. P. J., Fontijn, R. D., and Mul, P. (1987) *Eur. J. Biochem. 169*, 377−384.
10. Surerus, K. K., Chen, M., Van der Zwaan, J. W., Rusnak, F. M., Kolk, M., Duin, E. C., Albracht, S. P. J., and Münck, E. (1994) *Biochemistry 33*, 4980−4993.
11. Rakhely, G., Colbeau, A., Garin, J., Vignais, P. M., and Kovacs, K. L. (1998) *J. Bacteriol. 180*, 1460−1465.
12. Volbeda, A., Charon, M.-H., Piras, C., Hatchikian, E. C., Frey, M., and Fontecilla-Camps, J. C. (1995) *Nature 373*, 580−587.
13. Volbeda, A., Garcin, E., Piras, C., de Lacey, A., Fernandez, V. M., Hatchikian, E. C., Frey, M., and Fontecilla-Camps, J. C. (1996) *J. Am. Chem. Soc. 118*, 12989−12996.
14. Fontecilla-Camps, J. C., Frey, M., Garcin, E., Hatchikian, E. C., Montet, Y., Piras, C., Vernède, X., and Volbeda, A. (1997) *Biochimie 79*, 661−666.
15. Rousset, M., Montet, Y., Guigliarelli, B., Forget, N., Asso, M., Bertrand, P., Fontecilla-Camps, J. C., and Hatchikian, E. C. (1998) *Proc. Natl. Acad. Sci. U.S.A. 95*, 11625−11630.
16. Armstrong, F. A., Heering, H. A., and Hirst, J. (1997) *Chem. Soc. Rev. 26*, 169.
17. Armstrong, F. A. (1997) in *Bioelectrochemistry of biomacromolecules* (Lenaz, G., and Milazzo, G., Eds.) Birkhäuser Verlag, Basel, Switzerland.
18. Sucheta, A., Ackrell, B. A. C., Cochran, B., and Armstrong, F. A. (1992) *Nature 356*, 361−362.
19. Sucheta, A., Cammack, R., Weiner, J., and Armstrong, F. A. (1993) *Biochemistry 32*, 5455−5465.
20. Heering, H. A., Weiner, J. H., and Armstrong, F. A. (1997) *J. Am. Chem. Soc. 119*, 11628−11638.
21. Heering, H. A., Hirst, J., and Armstrong, F. A. (1998) *J. Phys. Chem. B 102*, 6889−6902.
22. Hirst, J., Sucheta, A., Ackrell, B. A. C., and Armstrong, F. A. (1996) *J. Am. Chem. Soc. 118*, 5031.
23. Hirst, J., Ackrell, B. A. C., and Armstrong, F. A. (1997) *J. Am. Chem. Soc. 119*, 7434.
24. Mondal, M. S., Fuller, H. A., and Armstrong, F. A. (1996) *J. Am. Chem. Soc. 118*, 263.
25. Mondal, M. S., Goodin, D. B., and Armstrong, F. A. (1998) *J. Am. Chem. Soc. 120*, 6270−6276.
26. Van Heerikhuizen, H., Albracht, S. P. J., Slater, E. C., and Van Rheenen, P. S. (1981) *Biochim. Biophys. Acta 657*, 26−39.
27. Albracht, S. P. J., Kalkman, M. L., and Slater, E. C. (1983) *Biochim. Biophys. Acta 724*, 309−316.
28. Hendly, D. D. (1955) *J. Bacteriol. 70*, 625−634.
29. Coremans, J. M. C. C., Van der Zwaan, J. W., and Albracht, S. P. J. (1992) *Biochim. Biophys. Acta 1119*, 157−168.
30. Laemmli, U. K. (1970) *Nature 227*, 680−685.
31. Bradford, M. M. (1976) *Anal. Biochem. 72*, 248−254.
32. Bard, A. J., and Faulkner, L. R. (1980) *Electrochemical Methods, Fundamentals and Applications*, Wiley, New York.
33. Heering, H. A., Mondal, M. S., and Armstrong, F. A. (1999) *Anal. Chem. 71*, 174−182.
34. Armstrong, F. A., Butt, J. N., and Sucheta, A. (1993) *Methods Enzymol. 227*, 479−500.
35. Butt, J. N., Filipiak, M., and Hagen, W. R. (1997) *Eur. J. Biochem. 245*, 116−122.
36. Lissolo, T., Pulvin, S., and Thomas, D. (1984) *J. Biol. Chem. 259*, 11725−11729.
37. Coremans, J. M. C. C., Van der Zwaan, J. W., and Albracht, S. P. J. (1989) *Biochim. Biophys. Acta 997*, 256−267.
38. Coremans, J. M. C. C., Van Garderen, C. J., and Albracht, S. P. J. (1992) *Biochim. Biophys. Acta 1119*, 148−156.
39. Bianco, P., and Haladjian, J. (1992) *J. Electrochem. Soc. 139*, 2428−2432.
40. Bond, A. M. (1992) *Anal. Proc. 29*, 132−148.
41. Bond, A. M. (1993) *Analyst 118*, 973−978.
42. Turner, K., Doherty, M. K., Heering, H. A., Armstrong, F. A., Reid, G. A., and Chapman, S. K. (1999) *Biochemistry 38*, 3302−3309.
43. Clark, R. A., and Bowden, E. F. (1997) *Langmuir 13*, 559−565.
44. Egodage, K. L., deSilva, B. S., and Wilson, G. S. (1997) *J. Am. Chem. Soc. 119*, 5295−5301.
45. Nahir, T. M., and Bowden, E. F. (1996) *J. Electroanal. Chem. 410*, 9−13.
46. Mayhew, S. G. (1978) *Eur. J. Biochem. 85*, 535−547.
47. Teixeira, M., Moura, I., Xavier, A. V., Moura, J. J. G., LeGall, J., DerVartanian, D. V., Peck, H. D., Jr., and Huynh, B.-H. (1989) *J. Biol. Chem. 264*, 16435−16450.
48. Armstrong, F. A. (1997) *J. Bioinorg. Chem. 2* 139−142.
49. Cammack, R., Patil, D., Aguirre, R., and Hatchikian, E. C. (1982) *FEBS Lett. 142*, 289−292.
50. Pershad, H. R., Hirst, J., Cochran, B., Ackrell, B. A. C., and Armstrong, F. A. (1999) *Biochim. Biophys. Acta* (in press).

BI990108V